

# Template induced sol–gel synthesis of highly ordered LaNiO<sub>3</sub> nanowires

Zhi Yang, Yi Huang, Bin Dong, Hu-Lin Li\*

*College of Chemistry and Chemical Engineering, Lanzhou University, No. 222, Tianshui South Road, Gansu Province, Lanzhou City 730000, People's Republic of China*

Received 5 December 2004; received in revised form 12 January 2005; accepted 24 January 2005

## Abstract

The highly ordered LaNiO<sub>3</sub> nanowires of the rare-earth perovskite-type composite oxide were controlled synthesized within a porous anodic aluminum oxide (AAO) template by means of sol–gel method using nitrate as raw materials and citric acid as chelating agent. The results of scanning electron microscopy (SEM) and transmission electron microscopy (TEM) revealed that the obtained LaNiO<sub>3</sub> nanowires had a uniform length and diameter, which were determined by the thickness and the pore diameter of the applied AAO template. The results of X-ray diffraction (XRD) and the selected-area electron diffraction (SAED) indicated that the LaNiO<sub>3</sub> nanowires were perovskite-type crystalline structures. Furthermore, X-ray photoelectron spectroscopy (XPS) and the energy dispersive X-ray (EDX) spectroscopy demonstrated that the stoichiometric LaNiO<sub>3</sub> was formed.

© 2005 Elsevier Inc. All rights reserved.

*Keywords:* LaNiO<sub>3</sub> nanowires; Sol–gel; Template synthesis

## 1. Introduction

Because of their restricted size and high surface area, one-dimensional nanomaterials exhibit novel physical properties and play an important role in fundamental research as well as practical application. Plenty of efforts have been expended on the synthesis of nanoscale materials of various compounds. Recently, much attention has been paid to the preparation of composite oxides nanowires for their interesting and distinctive physical and chemical properties that are different from those of conventional bulk materials. Several composite oxide nanowires such as La<sub>1-x</sub>Ca<sub>x</sub>MnO<sub>3</sub> [1], La<sub>0.67</sub>Ca<sub>0.33</sub>MnO<sub>3</sub> [2], LiNi<sub>0.5</sub>Mn<sub>0.5</sub>O<sub>2</sub> [3], LiMnO<sub>2</sub> [4], and LiCoO<sub>2</sub> [5] have been successfully synthesized. In this paper, we select perovskite-type composite oxide LaNiO<sub>3</sub> as a subject, which is well-known material and

which has thus received intensive investigations over the years.

Functional perovskite composite oxides such as LaNiO<sub>3</sub> and related compounds, are very promising materials due to their innovative use in advanced technologies. These perovskite-type oxides are active oxidation catalysts [6–8], conductive thin films [9–11] and electrode materials [12,13]. The synthesis of LaNiO<sub>3</sub> and related compounds have been achieved by many methods, including sol–gel [14–16], sonochemical synthesis [17], metalorganic decomposition [18], pulsed laser ablation [19], and metal-organic CVD method [20].

Recent publications mainly focus on the preparation and properties of the LaNiO<sub>3</sub> films and powders. In contrast, the investigations on wire-like LaNiO<sub>3</sub> nanostructures are quite limited. The properties of the final materials obtained are strongly dependent on the preparation method. Shankar et al. [2] have stated that the La<sub>0.67</sub>Ca<sub>0.33</sub>MnO<sub>3</sub> nanowires fabricated by AAO, a composite oxide nanowire, were ferromagnetic at room temperature and exhibited enhanced ferromagnetic

\*Corresponding author. Fax: +86 931 891 2582.

E-mail address: [lihl@lzu.edu.cn](mailto:lihl@lzu.edu.cn) (H.-L. Li).

transition temperature well in excess of 300 K, which was substantially higher than that of single crystalline  $\text{La}_{0.67}\text{Ca}_{0.33}\text{MnO}_3$ . For most applications, the controlled synthesis of homogeneity, high purity and high surface areas  $\text{LaNiO}_3$  materials is necessary for obtaining reproducible properties.  $\text{LaNiO}_3$  nanowires have higher surface areas compared to  $\text{LaNiO}_3$  films and powders, and hence should enhance the effectiveness of the material in many applications, e.g., catalysis and gas sensitivity. Up to now, the synthesis of nanowires of multi-component oxides is still a challenging issue.

As an important way to prepare one-dimensional nanomaterials, template methods have attracted more and more attention in preparing ordered carbon nanotube, semiconductor nanowire arrays, magnetic nanowire arrays, etc. As the pore density is high, the pore distribution is uniform and the diameter of the pores is easily controlled by anodizing conditions [21]; porous anodic alumina oxide (AAO) templates are considered as particularly attractive templates for fabricating nanowires. Sol–gel method has become a popular method for preparation of inorganic materials and has a number of advantages over more conventional synthetic procedures such as high purity, homogeneous multi-component and easy chemical doping of the materials prepared. Sol–gel deposition has been widely used to fabricate nanowire arrays in the nanochannels of the template [22,23]. This method typically entails hydrolysis of a solution of a precursor molecule to firstly obtain a suspension of colloidal particles (the sol) and then a gel composed of aggregated sol particles. The gel is then thermally treated to yield the desired material.

Herein we have perfectly combined the concepts of sol–gel synthesis and template preparation of nanomaterials for the first time to yield a novel general route for fabricating highly ordered  $\text{LaNiO}_3$  nanowires, which are distinctly different from the results of conventional methods. This was accomplished by conducting sol–gel synthesis within the pores of nanoporous membranes; mono-dispersed  $\text{LaNiO}_3$  nanowires were obtained. This process uses inexpensive raw materials and can be performed at room temperature.

## 2. Experimental section

### 2.1. Membrane preparation

High-purity aluminum foil (99.999%) employed in this experiment was ultrasonically degreased in acetone for 10 min, etched in  $1.0\text{ mol L}^{-1}$  NaOH at room temperature for 3 min to remove the native oxide, washed thoroughly with distilled water, electropolished in a mixed solution of  $\text{HClO}_4:\text{CH}_3\text{CH}_2\text{OH} = 1:4(\text{V/V})$  for 5 min to provide a smooth surface and promptly rinsed with distilled water. Afterwards, the resulted

clean aluminum foil was anodized at  $80\text{ V}_{\text{dc}}$  for 2 h in  $0.5\text{ mol L}^{-1}$  phosphoric acid solution. Each sample was then placed into saturated  $\text{HgCl}_2$  solution for 1 h to separate the template membrane from the aluminum substrate. The membrane was rinsed with distilled water and immersed in  $0.5\text{ mol L}^{-1}$   $\text{H}_3\text{PO}_4$  solution for about 15 min at 328 K in order to dissolve the barrier-type part of nanoholes on the bottom. The obtained AAO template had a highly ordered porous structure with very uniform and nearly parallel pores, which could be organized in an almost precise hexagonal structure. The AAO template was characterized by using atomic force microscopy (AFM, Solver P47, Russia) and SEM (JSM-5600LV, Japan).

### 2.2. Preparation of $\text{LaNiO}_3$ nanowires

The  $\text{LaNiO}_3$  perovskite precursors in this work were prepared by the citrate-based sol–gel method. Analytical grade lanthanum nitrate ( $\text{La}(\text{NO}_3)_3 \cdot 6\text{H}_2\text{O}$ ), nickel nitrate ( $\text{Ni}(\text{NO}_3)_2 \cdot 6\text{H}_2\text{O}$ ), citric acid ( $\text{C}_6\text{H}_8\text{O}_7 \cdot \text{H}_2\text{O}$ ) and ammonia water ( $\text{NH}_3 \cdot \text{H}_2\text{O}$ ) were used as raw materials. According to the stoichiometric composition reactants, specified amounts of  $\text{La}(\text{NO}_3)_3 \cdot 6\text{H}_2\text{O}$  and  $\text{Ni}(\text{NO}_3)_2 \cdot 6\text{H}_2\text{O}$  were first dissolved in deionized water, then an amount of citric acid was added to the above solution. The molar amount of citric acid was equal to the total molar amount of metal nitrates in the solution. Ammonia water was slowly added to adjust the pH value of the solution in the range of 6–7 and stabilize the nitrate–citrate solution. During this procedure, the solution was kept at a temperature of 333 K and continuously stirred. Thus a transparent and homogeneous sol was obtained.

The AAO template membrane was immersed into this sol for the desired amount of time and then removed. Excess sol on the membrane surface was wiped off using a laboratory tissue, followed by drying under vacuum at 323 K for 2 h. The membrane surface was carefully wiped again to remove salts crystallized on the surface and then heat treated at 923 K for 3 h in the open furnace. As a result,  $\text{LaNiO}_3$  nanowires were formed inside the pores of the AAO template.

### 2.3. Characterization of $\text{LaNiO}_3$ nanowires

The structure and morphology properties of  $\text{LaNiO}_3$  nanowires were characterized by several techniques. The SEM samples were obtained as follows: the alumina membrane was attached to an SEM sample stub with carbon conductive paint and then several drops of  $3\text{ mol L}^{-1}$  NaOH were added to the sample to dissolve the partial membrane. Prior to characterization, Au was sputtered onto the samples surface in order to increase their conductivity. The concentrations of La and Ni elements in the  $\text{LaNiO}_3$  nanowires were determined by

EDX analysis using a Kevex system (USA) attached to the above-mentioned scanning electron microscope. TEM images were obtained using a Hitachi-600 microscope. It was used to observe the morphology and degree of agglomeration of the nanowires. Before TEM observation, the alumina template membrane was dissolved by using  $3 \text{ mol L}^{-1}$  NaOH, and then diluted with distilled water for three times. Droplets of solution containing  $\text{LaNiO}_3$  nanowires were dropped onto the copper grids. The XRD patterns for  $\text{LaNiO}_3$  nanowires were recorded with a diffractometer (Rigaku D/MAX-2400, Japan) using  $\text{CuK}\alpha$  radiation ( $\lambda = 0.154184 \text{ nm}$ ). The current and voltage during the measurements were  $60 \text{ mA}$  and  $40 \text{ kV}$ , respectively. Scanning rate was  $10 \text{ min}^{-1}$  and the  $2\theta$  scanning range was from  $20^\circ$  to  $80^\circ$ . XPS data were obtained with a V.G. ESCA Lab. 2201-XL photoelectron spectrometer with  $\text{MgK}\alpha$  source, a concentric hemispherical analyzer operating in fixed analyzer transmission mode and a multi-channel detector. The pressure in the analysis chamber was less than  $2 \times 10^{-10} \text{ Torr}$ . The spectra were acquired with a  $50 \text{ eV}$  pass energy and a  $1 \text{ mm}^2$  spot (large area mode without using XL lens). The binding energy was calibrated with reference to the C  $1s$  level of carbon ( $284.8 \text{ eV}$ ).

### 3. Results and discussion

#### 3.1. Characterization of the membrane

When anodized in an acidic electrolyte, aluminum forms a porous oxide with very uniform and parallel pores open at one end and sealed at the other [21,24,25]. Its structure is described as a close-packed array of columnar cells, each containing a central pore of which the side and the interval can be controlled by changing the forming conditions [21,24,25]. As indicated in Fig. 1(a), the pores in the membrane are arranged in a regular hexagonal lattice. Perfect hexagonal pore arrays can be observed within domains of microsize, which are separated from neighboring aluminum oxide domains with a different orientation of the pore lattice by grain boundaries. Fig. 1(b) depicts the cross-section SEM image of the AAO template with pores parallel to each other and perpendicular to the surface of the membrane. Here, the pores of the membrane are about  $100 \text{ nm}$  in diameter and about  $50 \mu\text{m}$  in length with a pore density of about  $10^9\text{--}10^{10} \text{ cm}^{-2}$ .

#### 3.2. SEM and EDX analysis of $\text{LaNiO}_3$ nanowires

Fig. 2(a)–(c) shows SEM images of  $\text{LaNiO}_3$  nanowires grown in AAO template. These photographs show that the nanowires are uniformly distributed, highly ordered and parallel to each other. Few microscopic

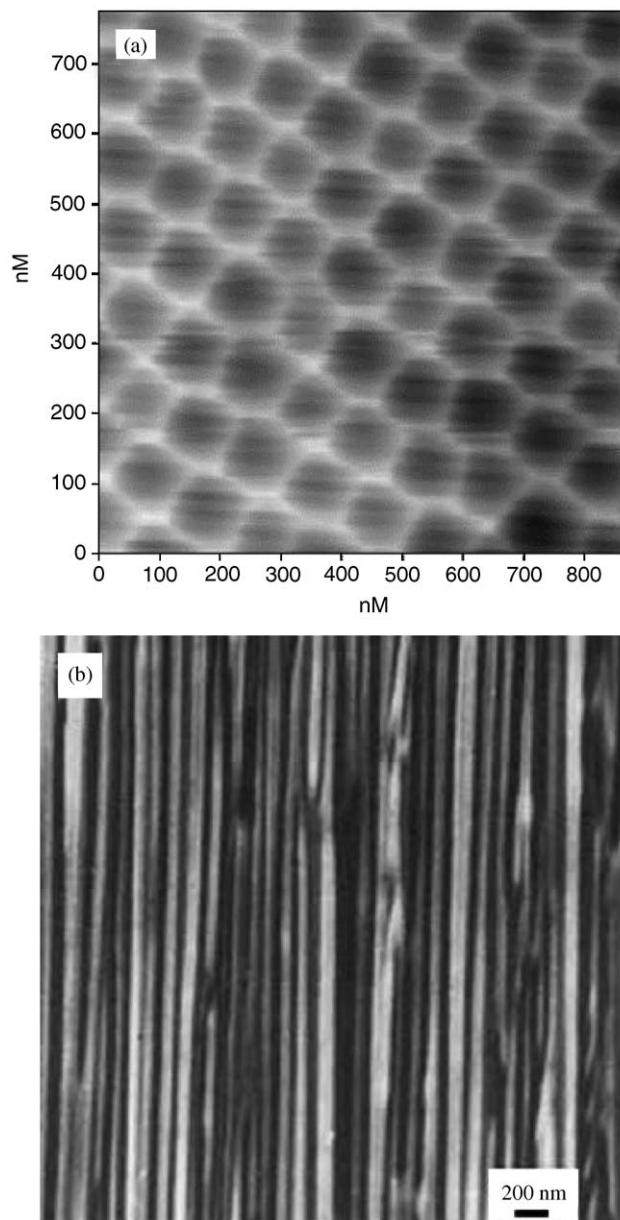


Fig. 1. (a) AFM image of the surface of AAO template under tapping mode and (b) SEM image of cross-section of AAO template.

defects are found in these wires. Figs. 2(a) and (b) are platforms from which we can find several clusters of nanowires. The clusters can result from the situation in which the nanowires are uncovered from the framework of the AAO template but freestanding incompletely. When the top alumina of the AAO template is dissolved away, the nanowires embedded in the template release gradually and incline to agglutinate together. It is conceivable that the surface energy of the nanowires causes this interesting phenomenon. Figs. 2(a) and (b) also show that  $\text{LaNiO}_3$  nanowires are abundant, uniform and highly ordered in a large area. Fig. 2(c) shows a split where the alumina matrix of the AAO

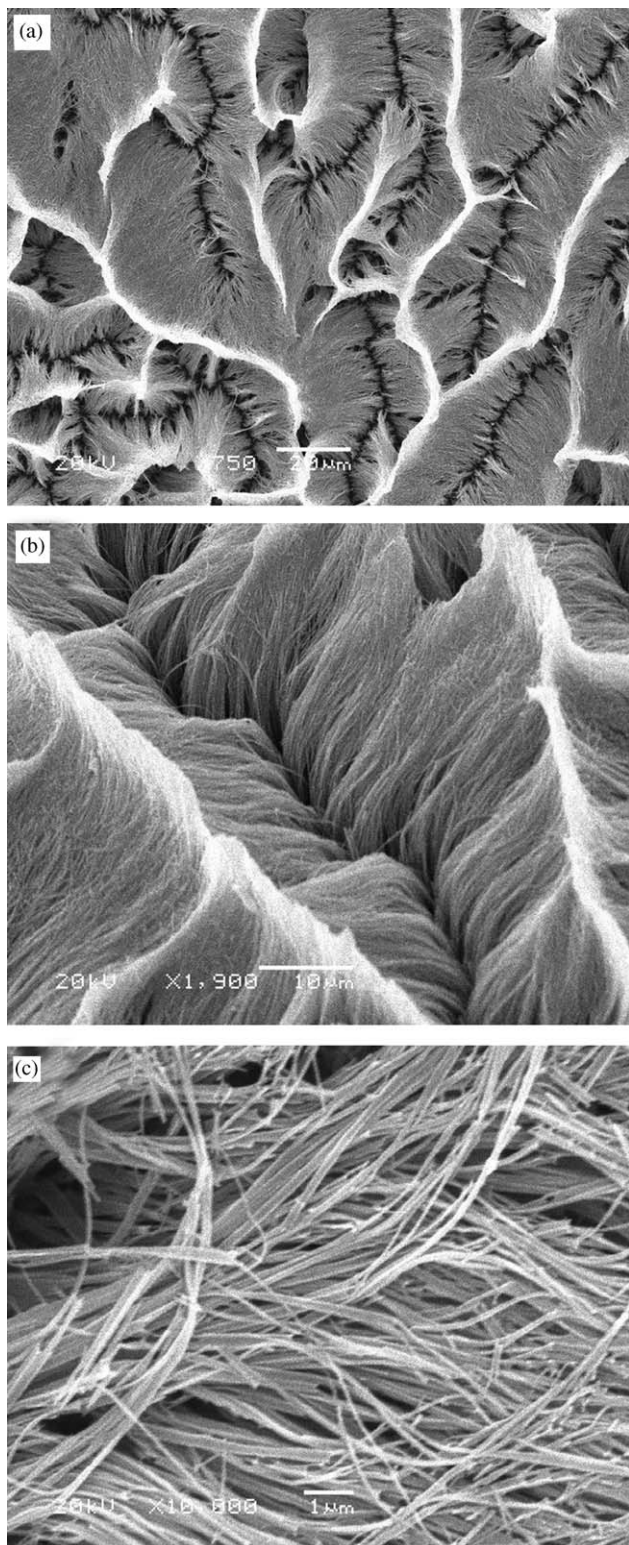


Fig. 2. SEM images of  $\text{LaNiO}_3$  nanowires with the AAO template partly dissolved: (a–b) top view in low magnification and (c) cross-section in high magnification.

template has been dissolved away and large quantities of  $\text{LaNiO}_3$  nanowires remain. It can be seen that the nanowires deposited inside the nanochannel of the AAO

template are parallel, tidily aligned and uniformly distributed. It is correlative to that the AAO template had an array of densely parallel nanoholes arranged in a hexagonal fashion. We can also see that these nanowires have a fiber-brush aspect. From these figures, we find that  $\text{LaNiO}_3$  nanowires can be produced in large areas within the pores of the AAO template. At the same time, it also can be estimated that the length of  $\text{LaNiO}_3$  nanowires is about  $50\ \mu\text{m}$ . It corresponds with the thickness of the AAO template. The outside diameters of these nanowires are about  $100\ \text{nm}$ , which are equivalent to the pore diameter of the template membrane.

In order to confirm the existence of  $\text{LaNiO}_3$  nanowires, EDX spectroscopy at the same position as Fig. 2(a) was done. As shown in Fig. 3 and Table 1, the sample contains La and Ni in addition to signals of alumina. The result shows the metal ratio La/Ni approximately equals 1:1. The percentage concentrations of La and Ni in the  $\text{LaNiO}_3$  nanowires determined by EDX agree with that obtained by stoichiometric analysis. The peak of element Au was obtained because Au was sputter covered on the surface in order to provide conductivity of the sample.

### 3.3. TEM and SAED analysis of $\text{LaNiO}_3$ nanowires

TEM images of  $\text{LaNiO}_3$  nanowires formed within the AAO template are shown in Figs. 4(a) and (b). Fig. 4(a) shows several  $\text{LaNiO}_3$  nanowires, in which some of these nanowires cross and overlap each other. This image also shows that the diameter of  $\text{LaNiO}_3$  nanowires is about  $100\ \text{nm}$ , which approximately equals those of the nanochannels of the employed AAO template. Although the lengths of nanowires are much less than  $50\ \mu\text{m}$ , it does not mean that the nanowires are only so short, because during the preparation of samples for TEM observation, the nanowires are easily broken by the ultrasonic stirring. These nanowires are uniformly distributed, which indicates that the alumina matrix is dissolved completely. Fig. 4(b) shows another image of two  $\text{LaNiO}_3$  nanowires. It can be seen that the surfaces of these nanowires are smooth. Fig. 4(c) shows the corresponding SAED pattern taken from  $\text{LaNiO}_3$  nanowires. Lots of individual  $\text{LaNiO}_3$  nanowires were characterized and we always observed diffraction rings. The SAED results indicate that  $\text{LaNiO}_3$  nanowires are polycrystalline. Generally, the nanowires prepared by the sol-gel method with the AAO templates are polycrystal [26,27]. It should be noted that the diffraction rings are discontinuous and consist of rather sharp spots, which indicates that the nanowires are well crystallized. According to the electron-diffraction formula, the major diffraction spots correspond to the (100), (110), (111), (200), (211), (220), and (310)

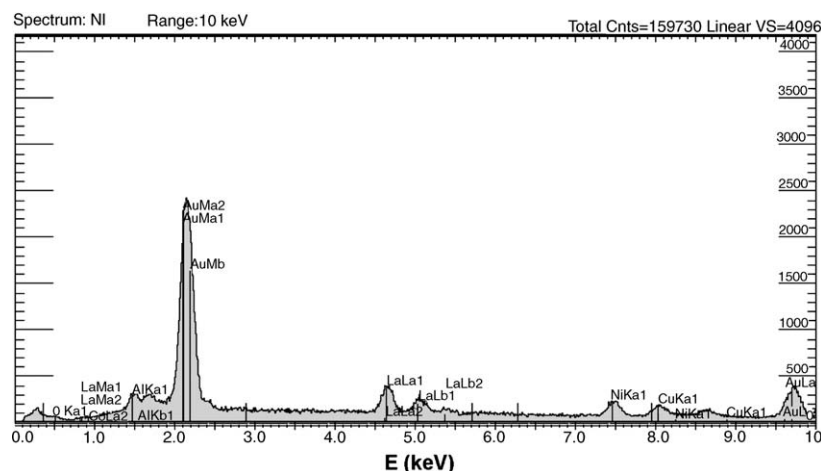


Fig. 3. EDX patterns of LaNiO<sub>3</sub> nanowires within the AAO template partly dissolved.

Table 1

The EDX elemental analysis results of LaNiO<sub>3</sub> nanowires within the AAO template

Element	Atomic%
La	36.5
Ni	36.9

diffraction planes for LaNiO<sub>3</sub> with cubic perovskite structure.

### 3.4. XRD analysis of LaNiO<sub>3</sub> nanowires

Fig. 5 shows the XRD patterns of LaNiO<sub>3</sub> nanowires after heat treatment at 923 K for 3 h. All the observed XRD peaks present sharp reflections, showing that the nanowires are well crystallized after all the temperature treatments. The peak positions and their relative intensities are consistent with the standard powder diffraction patterns of a cubic perovskite-type LaNiO<sub>3</sub> phase (JCPDS, card number: 33-0710). All of the diffraction peaks are assigned to LaNiO<sub>3</sub> and no other peaks attributable to La<sub>2</sub>O<sub>3</sub> and NiO are observed. The XRD patterns of LaNiO<sub>3</sub> nanowires are characteristic of crystalline perovskite oxides, with cubic cell, *Pm3m* space group [28].

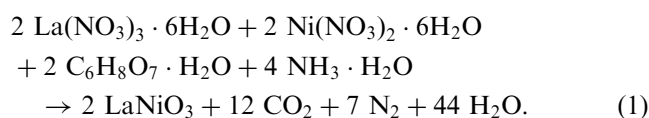
### 3.5. XPS analysis of LaNiO<sub>3</sub> nanowires

The oxidation state of principal elements of LaNiO<sub>3</sub> nanowires in the pores of AAO can be determined by XPS. The binding energies obtained in the XPS analysis are standardized for specimen charging using C 1s as the reference at 284.8 eV. Figs. 6(a)–(d) display the XPS spectra of La 3d<sub>5/2</sub>, Ni 2p, O 1s and Al 2p core levels for

LaNiO<sub>3</sub> nanowires embedded in AAO template, respectively. The line of the La 3d<sub>5/2</sub> core level has two binding energy peaks located at 838.9 and 835.8 eV (Fig. 6(a)). The peaks located at 855.5 and 873.9 eV (Fig. 6(b)) are attributed to the spin–orbit splitting of the Ni (2p) components, Ni (2p<sub>3/2</sub>) and Ni (2p<sub>1/2</sub>), respectively. The line shape of the core levels O 1s and Al 2p are Gaussian like with a binding energy of 530.4 eV (Fig. 6(c)) and 74.3 eV (Fig. 6(d)), respectively. We can see that the peak intensities of O 1s and Al 2p are higher than for the other elements. The reason for the weaker peak intensity of La 3d<sub>5/2</sub> and Ni 2p derives from the low concentration of LaNiO<sub>3</sub> in the AAO template and the LaNiO<sub>3</sub> not being covered on the surface of the template. The binding energy values for principal elements of LaNiO<sub>3</sub> in the pores of AAO are in good agreement with those of LaNiO<sub>3</sub> in literatures [29–31]. XPS spectra further confirm that the main composition of the nanowires in the pores of AAO is the stoichiometric LaNiO<sub>3</sub> material.

### 3.6. The mechanism of the fabrication of LaNiO<sub>3</sub> nanowires

The SAED, XRD and XPS data show that the LaNiO<sub>3</sub> nanowires are formed. The formation process of these nanowires can be described by the following [32]:



From Eq. (1), it can be seen that the reaction is an oxidation-reduction reaction, in which nitrate ions act as

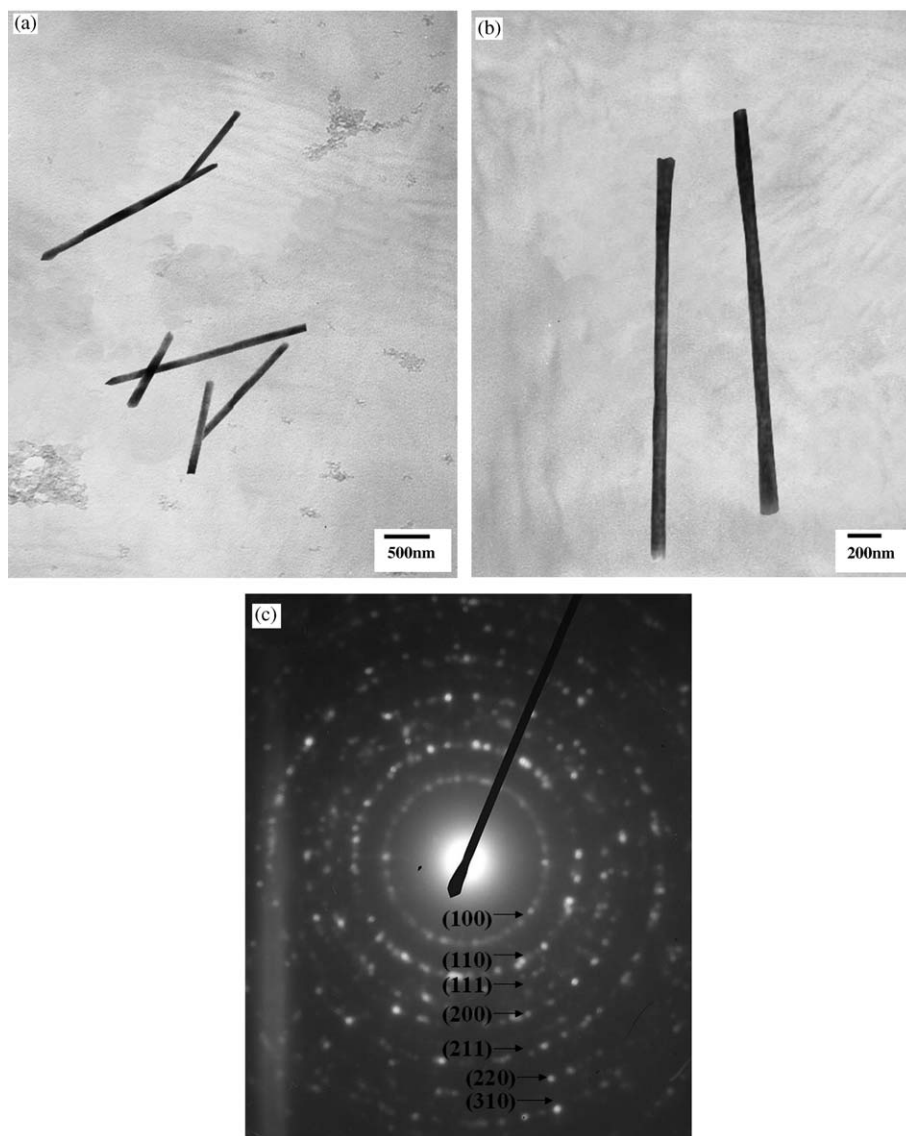


Fig. 4. (a) TEM image of several  $\text{LaNiO}_3$  nanowires after removing AAO, (b) TEM image of two  $\text{LaNiO}_3$  nanowires, and (c) the corresponding selected area electron diffraction for  $\text{LaNiO}_3$  nanowires.

oxidizers and the carboxyl group is reducing agent. Here, citric acid acts as chelating agent.

The fact that  $\text{LaNiO}_3$  nanowires are initially formed in the AAO template membrane indicated that the  $\text{LaNiO}_3$  sol particles adsorb to the porewalls of AAO membrane. It is reported that the sol particles are weakly positively charged, whereas the pore walls of AAO membranes are weakly cationic [33]. Hence, electrostatic interactions between the pore wall and the sol particles initially result in the formation of  $\text{LaNiO}_3$  nanowires. Then  $\text{LaNiO}_3$  nanowires are formed at 923 K. In this process the nanochannels of the AAO template acted as a micro-cell in which  $\text{LaNiO}_3$  nanowires were formed, shaped, and subsequently changed into the nanocrystalline perovskite oxides under high heat treatment temperature.

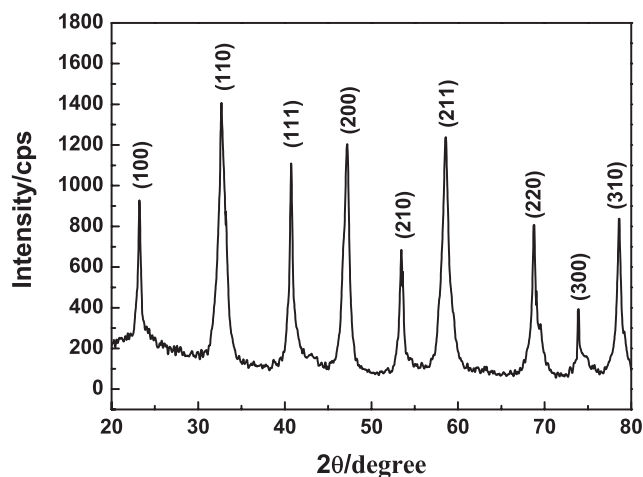


Fig. 5. XRD patterns of  $\text{LaNiO}_3$  nanowires.

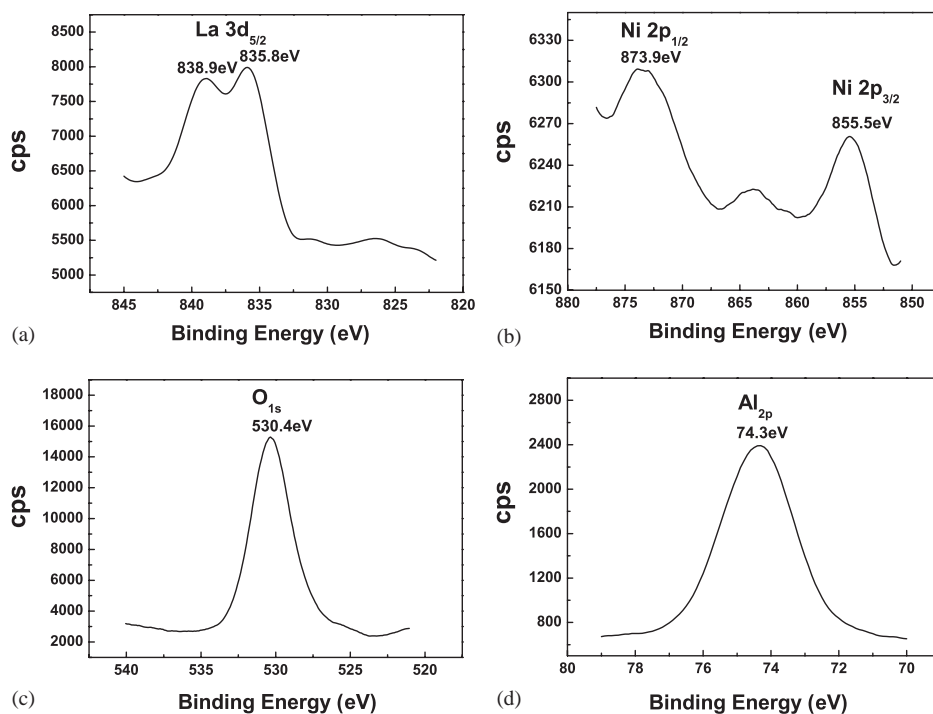


Fig. 6. XPS spectra of (a) La  $3d_{5/2}$ ; (b) Ni  $2p$ ; (c) O  $1s$  and (d) Al  $2p$  core levels for LaNiO<sub>3</sub>/AAO membrane.

#### 4. Conclusion

In summary, highly ordered LaNiO<sub>3</sub> nanowires were successfully fabricated by a citrate-based sol-gel template process. We have also applied SEM, EDX, TEM, XRD and XPS techniques to characterize the structure of LaNiO<sub>3</sub> nanowires. The SEM and TEM results showed that highly ordered LaNiO<sub>3</sub> nanowires had a uniform length and diameter, which were determined by the thickness and the pore diameter of the applied AAO template, respectively. XRD patterns indicated that perovskite-type LaNiO<sub>3</sub> nanowires were orthorhombic symmetry structures. The result of SAED demonstrated that LaNiO<sub>3</sub> nanowires were polycrystalline. XPS and EDX analysis demonstrated that the stoichiometric LaNiO<sub>3</sub> nanowires were formed. We have succeeded in providing a meaningful method to design perovskite-type composite oxides LaNiO<sub>3</sub> nanowires. It could be expected that the novel and effective technique presented in this article would be also appropriate for the preparation of nanowires of other mono-component or multi-component oxides. This facile method of preparing highly ordered LaNiO<sub>3</sub> nanowires with a large area might be important for many applications in nanomaterials.

#### Acknowledgments

This work is supported by the National Natural Science Foundation of China (No. 60471014). The

authors would like to express their sincere thanks to Researcher Jia-Zheng Zhao of Lanzhou Institute of Chemical Physics of the Chinese Academy of Sciences for SEM measurement.

#### References

- [1] X.Y. Ma, H. Zhang, J. Xu, J.J. Niu, Q. Yang, J. Sha, D.R. Yang, *Chem. Phys. Lett.* 363 (2002) 579–582.
- [2] K.S. Shankar, S. Kar, A.K. Raychaudhuri, G.N. Subbanna, *Appl. Phys. Lett.* 84 (2004) 993–995.
- [3] Y.K. Zhou, H.L. Li, *J. Mater. Chem.* 12 (2002) 681–686.
- [4] Y.K. Zhou, J.E. Huang, H.L. Li, *Appl. Phys. A: Mater. Sci. Process.* 76 (2003) 53–57.
- [5] Y.K. Zhou, C.M. Shen, H.L. Li, *Solid State Ionics* 146 (2002) 81–86.
- [6] J.J. Guo, H. Lou, Y.H. Zhu, X.M. Zheng, *Mater. Lett.* 57 (2004) 4450–4455.
- [7] J.J. Guo, H. Lou, Y.H. Zhu, X.M. Zheng, *J. Nat. Gas Chem.* 12 (2003) 17–22.
- [8] H. Li, Q. Liang, L.Z. Gao, S.H. Tang, Z.Y. Cheng, B.L. Zhang, Z.L. Yu, C.F. Ng, C.T. Au, *Catal. Lett.* 74 (2001) 185–188.
- [9] K.P. Rajeev, G.V. Shivashankar, A.K. Raychaudhuri, *Solid State Commun.* 79 (1991) 591–595.
- [10] S.H. Yu, K. Yao, F.E.H. Tay, *Chem. Mater.* 16 (2004) 346–350.
- [11] T.J. Zhu, L. Lu, *J. Appl. Phys.* 95 (2004) 241–247.
- [12] D. Hesse, N.D. Zakharov, A. Pignolet, A.R. James, S. Senz, *Cryst. Res. Technol.* 35 (2000) 641–651.
- [13] T. Yu, Y.F. Chen, Z.G. Liu, S.B. Xiong, L. Sun, X.Y. Chen, N.B. Ming, *Mater. Lett.* 26 (1996) 291–294.
- [14] S. Miyake, S. Fujihara, T. Kimura, *J. Eur. Ceram. Soc.* 21 (2001) 1525–1528.
- [15] H. Provendier, C. Petit, J.L. Schmitt, A. Kienemann, C. Chaumont, *J. Mater. Sci.* 34 (1999) 4121–4127.

- [16] G.J. Zhang, R. Liu, Y. Yang, Y.Q. Jia, *Phys. Stat. Sol. A* 160 (1997) 19–27.
- [17] X.Y. Liang, Z. Ma, Z.C. Bai, Y.N. Qin, *Acta Phys. Chim. Sin.* 18 (2004) 567–571.
- [18] A.D. Li, D. Wu, Z.G. Liu, C.Z. Ge, X.Y. Liu, G.X. Chen, N.B. Ming, *Thin Solid Films* 336 (2004) 386–390.
- [19] T. Yu, Y.F. Chen, Z.G. Liu, X.Y. Chen, L. Ming, N.B. Sun, L.J. Shi, *Mater. Lett.* 26 (1996) 73–76.
- [20] A.L. Penelope, J.C. Michael, J.W. Peter, P.D. Paul, J.H. Philip, L.R. Christopher, J.A. Carl, C.J. Jason, A.T. Michael, J.W. Dennis, *Chem. Vapor Deposit.* 9 (2003) 87–92.
- [21] C.A. Huber, T.E. Huber, M. Sadoqi, J.A. Lubin, S. Manalis, C.B. Prater, *Science* 263 (1994) 800–802.
- [22] B.B. Lakshmi, P.K. Dorhout, C.R. Martin, *Chem. Mater.* 9 (1997) 857–862.
- [23] M. Ohyama, H. Kozuma, T. Yoko, *J. Am. Ceram. Soc.* 81 (1998) 1622–1632.
- [24] Y. Peng, H.L. Zhang, S.L. Pan, H.L. Li, *J. Appl. Phys.* 87 (2000) 7405–7408.
- [25] S.L. Pan, H.L. Zhang, Y. Peng, Z. Wang, H.L. Li, *Chem. J. Chin. Univ.* 20 (1999) 1622–1624.
- [26] Y. Lin, F.Q. Sun, X.Y. Yuan, B.Y. Geng, L.D. Zhang, *Appl. Phys. A: Mater. Sci. Process.* 78 (2003) 1197–1199.
- [27] B.A. Hernandez, K.S. Chang, E.R. Fisher, P.K. Dorhout, *Chem. Mater.* 14 (2002) 480–482.
- [28] E. Bontempi, C. Garzella, S. Valetti, L.E. Depero, *J. Eur. Ceram. Soc.* 23 (2003) 2135–2142.
- [29] P. Xue, Y.Z. Gao, *Rare Earth* 18 (1997) 51–54.
- [30] H. Seim, H. Molsa, M. Nieminen, H. Fjellvag, L. Niinisto, *J. Mater. Chem.* 7 (1997) 449–454.
- [31] J. Choisnet, N. Abadzhieva, P. Stefanov, D. Klissurski, J.M. Bassat, V. Rives, L. Minchev, *J. Chem. Soc.—Faraday Trans.* 90 (1994) 1987–1991.
- [32] X.W. Qi, J. Zhou, Z.X. Yue, Z.L. Gui, L.T. Li, *Mater. Chem. Phys.* 78 (2002) 25–29.
- [33] B.B. Lakshmi, C.J. Patrisi, C.R. Martin, *Chem. Mater.* 9 (1997) 2544–2550.